

1 (W)hole new field: the new GEM Time Projection 2 Chamber of ALICE

3 **Dariusz Miśkowiec on behalf of the ALICE Collaboration**

4 GSI Helmholtzzentrum für Schwerionenforschung, Planckstr. 1, 64291 Darmstadt, Germany

5 E-mail: d.miskowiec@gsi.de

6 **Abstract.** The ALICE Time Projection Chamber has just been upgraded by replacing the
7 readout chambers, which cover the two ends of the cylinder, with new detectors based on
8 the Gas Electron Multiplier (GEM) technology. We report here on the related activities at
9 GSI Darmstadt: GEM framing and chamber production, as well as the quality assurance
10 accompanying both procedures.

11 1. Introduction

12 The ALICE Time Projection Chamber (TPC) (Fig. 1) is the world's largest detector of its
13 kind [1]. It served as the main central tracking and particle-identification detector of ALICE
14 from 2009 till now (see Refs. [2] and [3] for the description of the experiment and its performance).

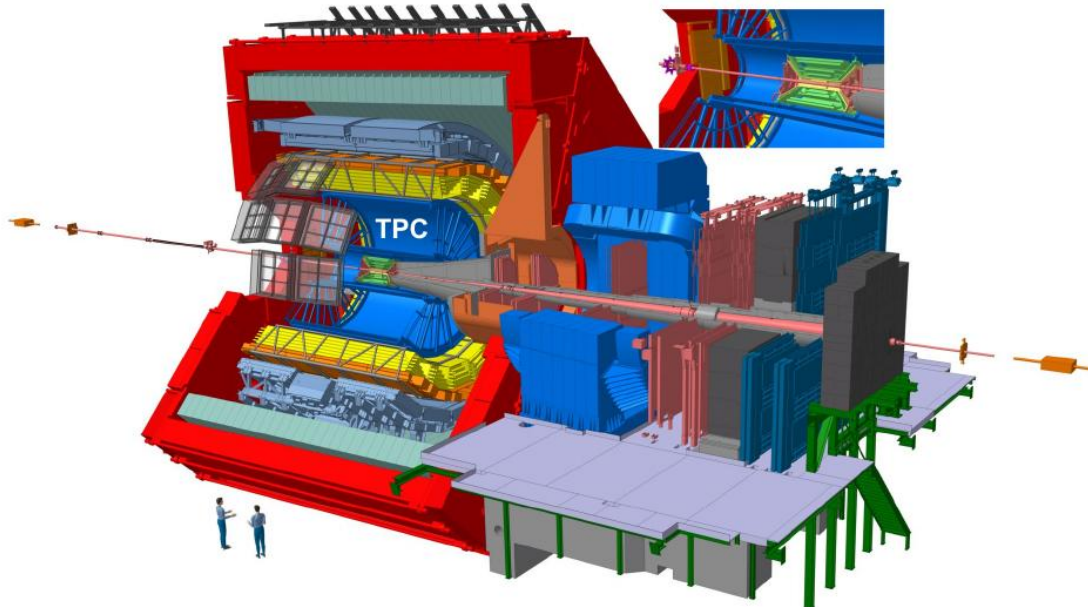


Figure 1. The ALICE apparatus at the CERN LHC. The Time Projection Chamber is the main tracking and particle identification detector of the ALICE central barrel.

15 Its upgrade is an essential part of the experiment's preparation for the LHC Run 3 starting in
 16 2021, when the machine will deliver Pb–Pb collisions at a rate of 50 kHz [4, 5].

17 The principle of operation of the ALICE TPC as used in Runs 1 and 2 is as follows. The
 18 TPC is filled with Ne-CO₂-N (90-10-5). Charged particles traversing its drift volume ionize gas
 19 atoms. An electric field of 400 V/cm makes the ionization electrons drift towards the readout
 20 chambers (Fig. 2) in which the charges are amplified and produce measurable signals. The
 21 nominal gas amplification factor is 7000–8000. The ions produced during the amplification
 22 slowly drift towards the cathode and, if not stopped, would result in a space charge within the
 23 active volume. The space charge would affect the electron drift in the subsequent events. In
 24 order to avoid this, a dedicated wire plane (gating grid) is located at the boundary between
 25 the drift volume and the readout chambers. About 100 μ s after every trigger, after the last
 26 ionization electrons have arrived to the readout chambers but before the first ions reach the
 27 drift volume, the gating grid is made opaque by applying alternating voltages to its wires. The
 28 gating grid is kept closed for 180 μ s. This method solves the problem of ion backflow, at the
 expense of introducing a significant downtime limiting the trigger rate to about 3 kHz.

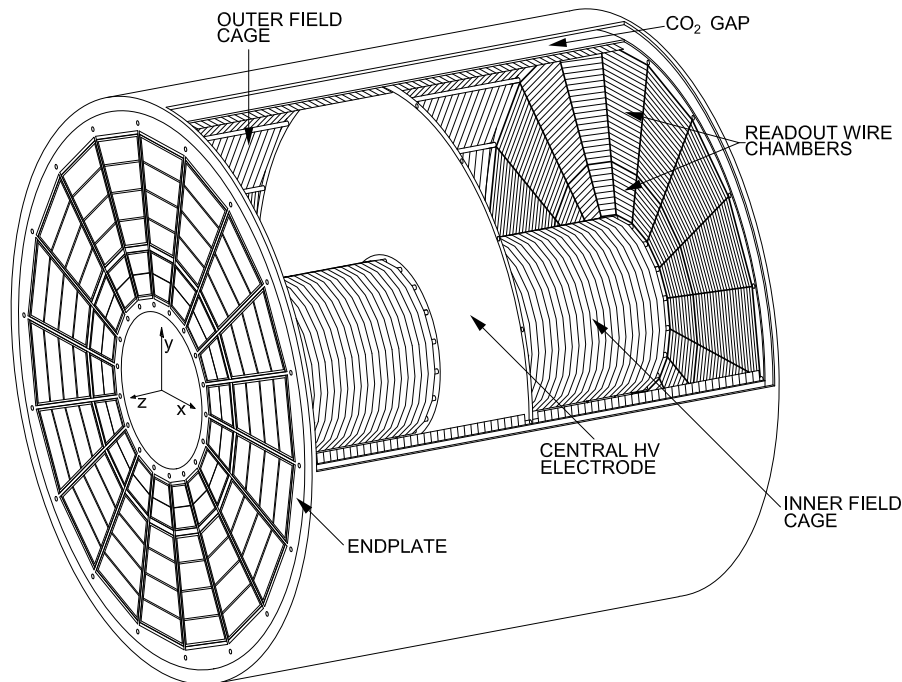


Figure 2. The ALICE Time Projection Chamber. The ionization electrons drift parallel to the cylinder axis towards its ends, where they are amplified and produce signals in the readout chambers. With a segmentation of 20° in azimuth and two sizes in radial direction, there are 36 inner and 36 outer readout chambers (IROCs and OROCs). These chambers have just been replaced by GEM-based chambers. Half of the new OROCs was assembled and tested at GSI.

29 The ongoing upgrade of the CERN accelerators will allow for Pb–Pb collision rates of 50 kHz
 30 from 2021 on. In order to fully make use of this, the readout chambers of the ALICE TPC
 31 have just been replaced by chambers of similar geometry but without the gating grid. Also
 32 the cathode and anode wire planes have been removed, the gas amplification is now performed
 33 sequentially in four layers of GEMs. Most of the ions are thus produced at the last GEM layer,
 34 and their way to the drift volume is made difficult by the presence of the first three GEM foils.
 35

36 With 8 potentials to tweak and with a somewhat reduced total gain factor, configurations can
 37 be found that result in an acceptable ion backflow ($<1\%$) while preserving the energy resolution
 38 (12% for 5.9 keV x-rays). The parameters of wire and GEM chambers are compared in Table 1.
 39 After eliminating the gating grid and the related dead time, the plan is to run the upgraded TPC
 40 in a continuous – rather than triggered – readout mode, thus recording all Pb–Pb interactions
 41 offered by the LHC.

Table 1. Comparison of wire and GEM chambers.

	wire chamber		GEM chamber
	grid open	grid closed	
gain	8000	0	2000
ion backflow	0.13	< 0.0001	< 0.01

42

43 2. GEM-chamber production

44 The ALICE TPC Upgrade collaboration consists of teams from 52 institutions. The chamber
 45 production was highly decentralized (Fig. 3). The GSI team joined the detector building
 46 activities in 2015, getting involved in GEM framing as well as assembly and tests of OROCs.
 47 The relevant steps of the production scheme are described below.

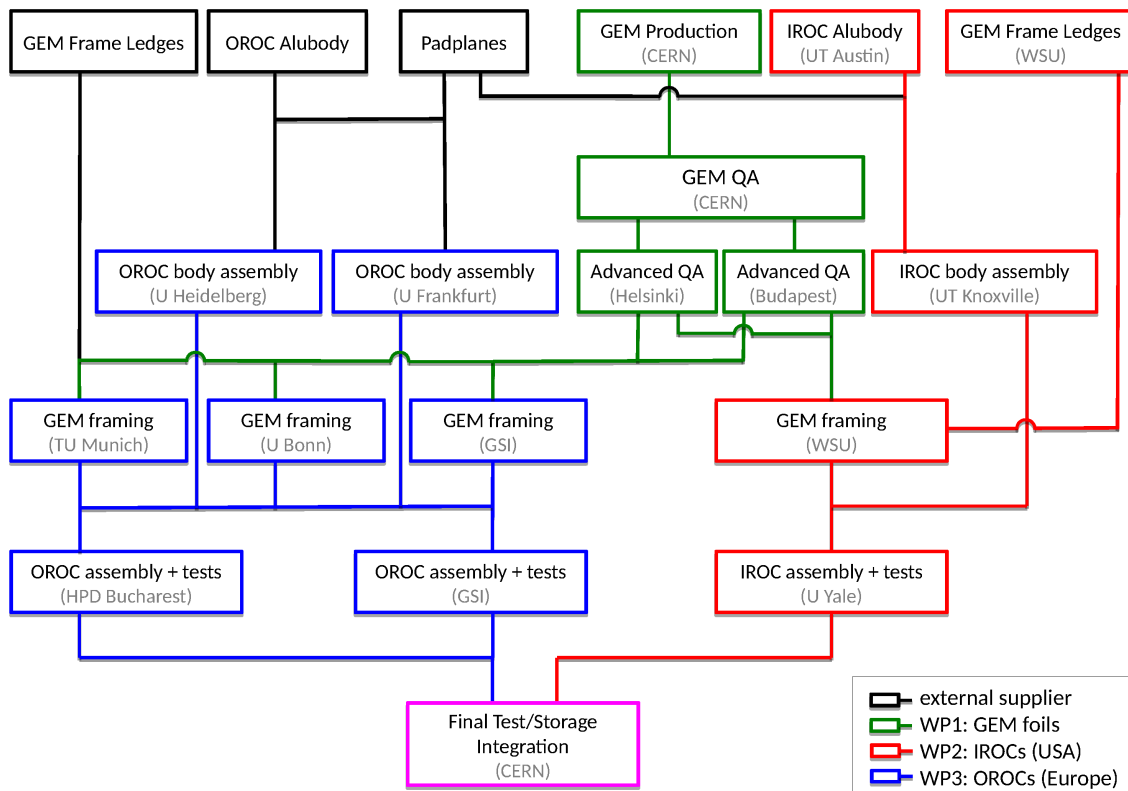


Figure 3. Scheme of GEM-chamber production project. The GSI team framed the largest GEM foils and assembled and tested 50% of the Outer Readout Chambers (OROCs).

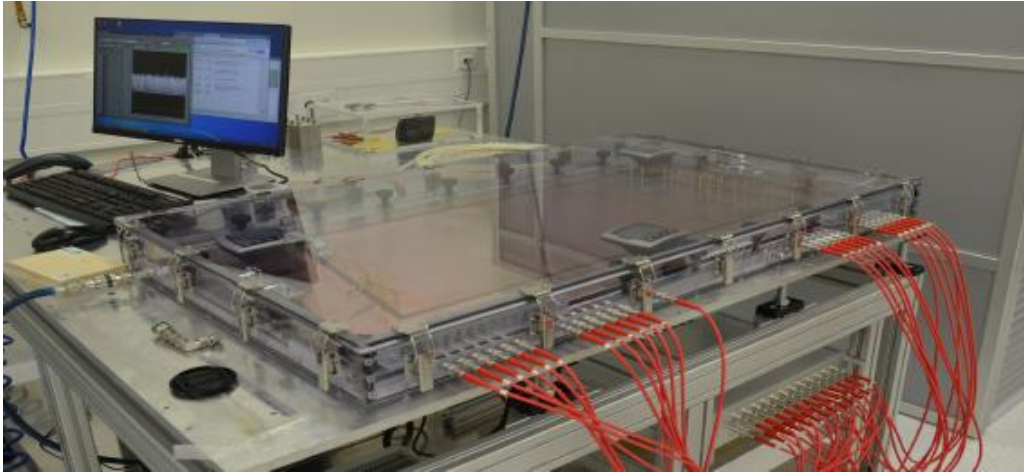


Figure 4. Measurement of the GEM dark current. The box is flushed with nitrogen, 500 V are applied and the currents are measured separately for all segments.

48 A basic test of a GEM, as performed in particular before and after every transport, consisted
49 in measuring its dark current. For this, a dry GEM (a few days spent at a relative humidity
50 $<1\%$) was placed in a plexiglass box equipped with spring-loaded pin contacts, and flushed
51 with nitrogen (Fig. 4). A voltage of 500 V was applied to all segments (20–24, depending on
52 GEM size) and the respective currents were monitored. Typically, the currents stabilized at a
53 level of 10–50 pA, depending on the hole pitch of a GEM. The currents of individual segments
54 within a GEM normally agreed within 10%. An excessive current of a segment meant a shorted
55 GEM. Increased current (see example in Fig. 5) may come from a defect/contamination and was

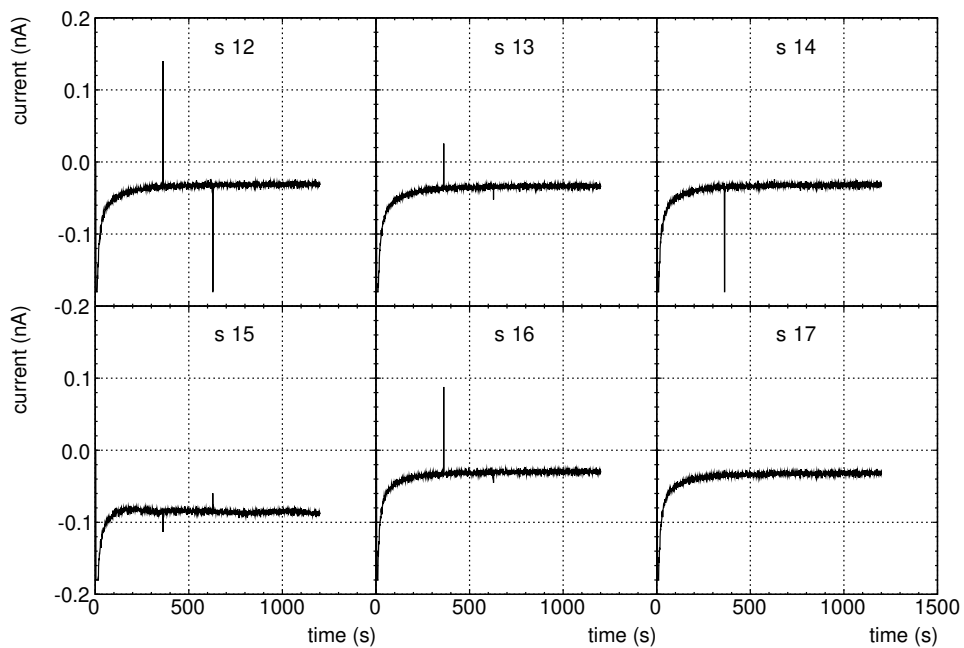


Figure 5. Example of a pathological GEM. Segment 15 (lower left panel) has a significantly higher current than others.

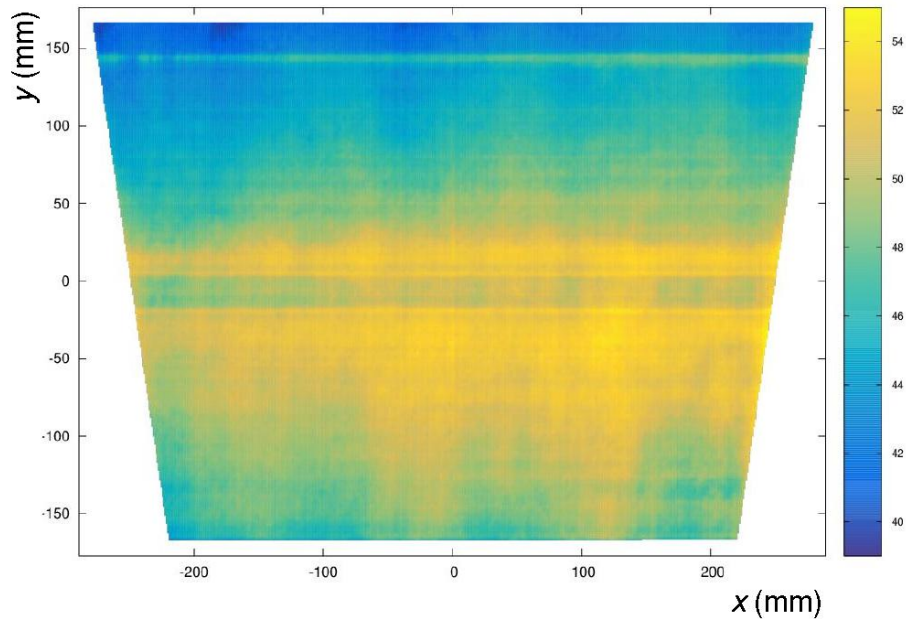


Figure 6. Example of a hole size map, extracted from optical survey of a GEM.

56 considered a potential danger. Shorted and contaminated GEMs had a fair chance of recovery
 57 when sent back to their production site for recleaning.

58 An advanced quality assurance procedure, performed once for each GEM, consisted in a
 59 long-term (at least 5 hours) dark-current measurement and an optical survey. During the latter,
 60 microscope photographs were taken of the entire GEM. The pictures were stitched together and
 61 analyzed for defects and hole-size nonuniformities (Fig. 6). The gain of a single GEM appeared
 62 to be clearly anticorrelated with the diameter of the holes. This correlation, however, was
 63 practically lost in a stack of four GEMs.

64 Framing a GEM consisted in stretching it and positioning 0.5 mm above a rigid frame made
 65 of G11 with a thin layer of epoxy glue on it. After a careful alignment (Fig. 7), the GEM foil
 66 was pressed to the frame and covered with a plexiglass hood. The box was flushed with nitrogen

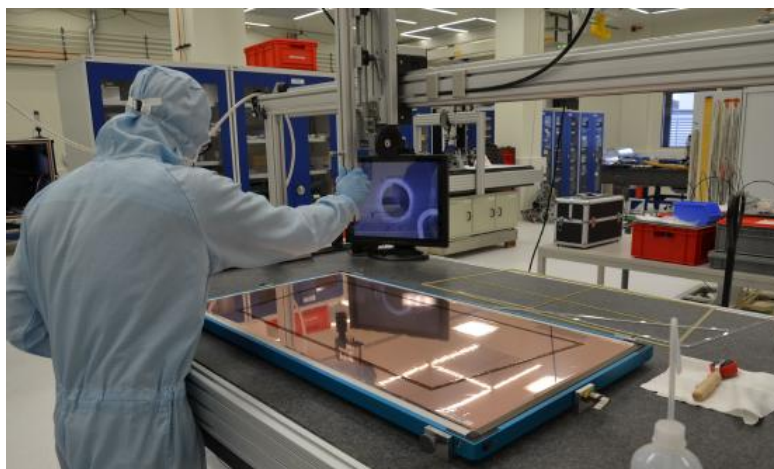


Figure 7. The GEM foil is being aligned to the epoxy-covered frame which is underneath it.

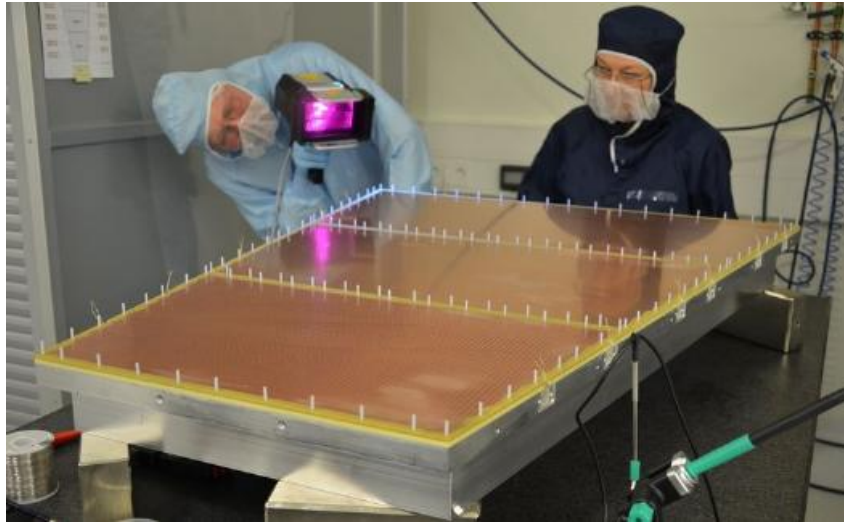


Figure 8. Chamber body before GEM installation. Readout pad planes of the three stacks and nylon bolts for GEM mounting are visible. The pad planes are inspected under UV light.

67 and left overnight.

68 The complete information about the 923 GEM foils of the project was stored in a dedicated
69 database. With an intuitive user interface and numerous analysis macros, the database was a
70 valuable tool in steering and monitoring the production process.

71 The OROC chamber assembly consisted in adding three stacks of 4 GEMs each to the chamber
72 bodies (Figs. 8, 9). The bodies were equipped with pad planes and connection wires bringing
73 HV into the chambers and the signals out of it. The GEMs were attached to them with densely
74 spaced nylon bolts (Fig. 8), ensuring a reasonable level of tension. The GEMs were trimmed to
75 trapezoidal shape and mounted one by one. The HV connections were soldered to both sides of
76 each GEM. As anticipated, the size, shape, and precise location of the soldering points were of
77 high importance for the HV stability of the chambers.



Figure 9. Chamber assembly. A GEM is being added to the stack. After adding the fourth – last – GEM foil, the nylon nuts holding stacks together are tightened with a torque of 6 Ncm.

3. GEM-chamber quality assurance

The chambers were subject to several tests at the assembly site. For this, they were enclosed in a test box filled with the nominal gas mixture, with a low-mass entrance windows and a 13 mm drift gap with 400 V/cm before the first GEM. The gain of the chamber, for each of the three GEM stacks separately, was measured by irradiating it with 5.9 keV x-rays from a ^{55}Fe source. The photons that reach the drift gap ionize gas atoms, producing on average a primary charge of 166 electrons. The absolute gain factor is calculated by dividing the pad current by the x-ray rate (measured using a scaler) and the primary charge. An example of the obtained gain curves is shown in Fig. 10.

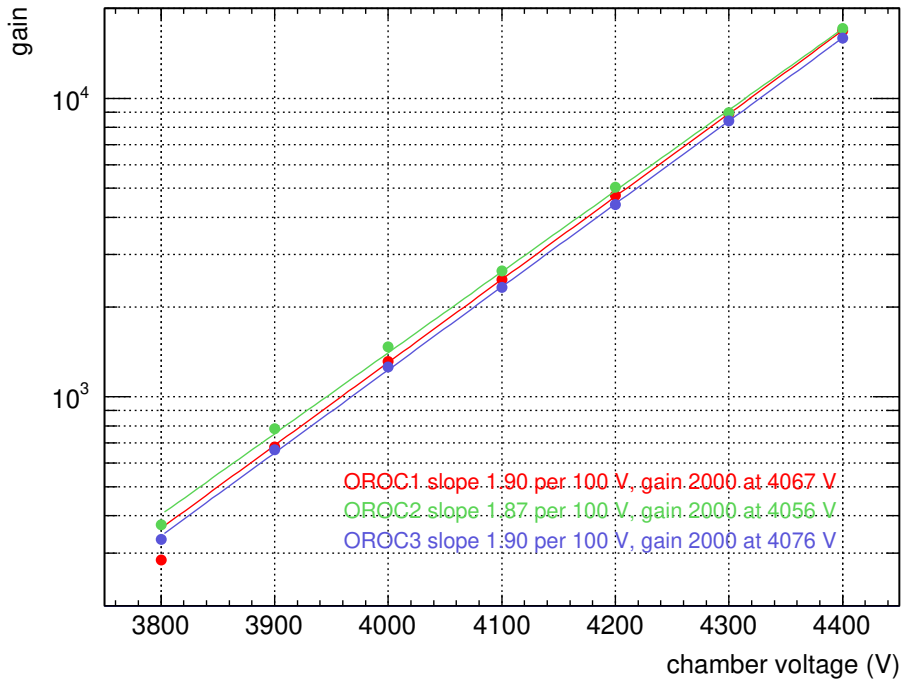


Figure 10. Gain curves of the three GEM stacks of one particular chamber (OROC/23). As expected, the gain increases exponentially with the applied voltage. The difference between stacks can be compensated by applying slightly different voltages. The nominal gain is 2000.

The charge induced on the pads is proportional to the primary ionization and thus to the energy deposited by the traversing charged particle. The energy resolution is checked by recording the ^{55}Fe x-ray spectrum and fitting the 5.9 keV peak (Fig. 11). The test is performed at a voltage corresponding to a gain of 2000. The relative width of the peak, calculated taking into account the position and the width of the pedestal, was typically around 12-14%, usually slightly above the limit of 12%. As the energy resolution and the ion backflow can be traded against each other by changing the GEM voltages, and as we notoriously observed an ion backflow significantly better than the limit, the poor values of the energy resolution were not considered to be a problem.

The gain homogeneity was evaluated by shifting a collimated x-ray tube over the chamber surface and monitoring the anode current (sum of all pads). This test was performed with the three stacks kept at a voltage corresponding to a gain of 2000. An example of the resulting current map is shown in Fig. 12.

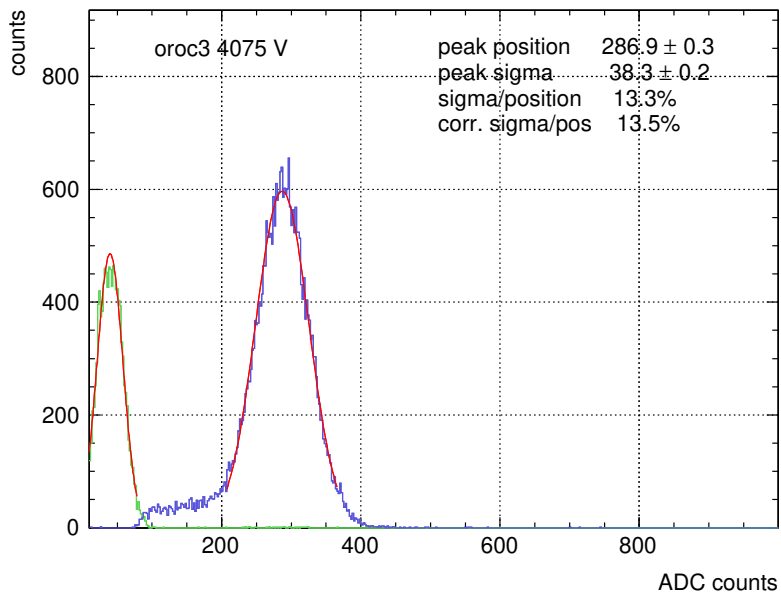


Figure 11. X-ray spectrum of ^{55}Fe , measured with the third stack of chamber OROC/23. The relative width of the 5.9 keV peak, corrected for the position and width of the pedestal (smaller peak on the left side), is the measure of the energy resolution.

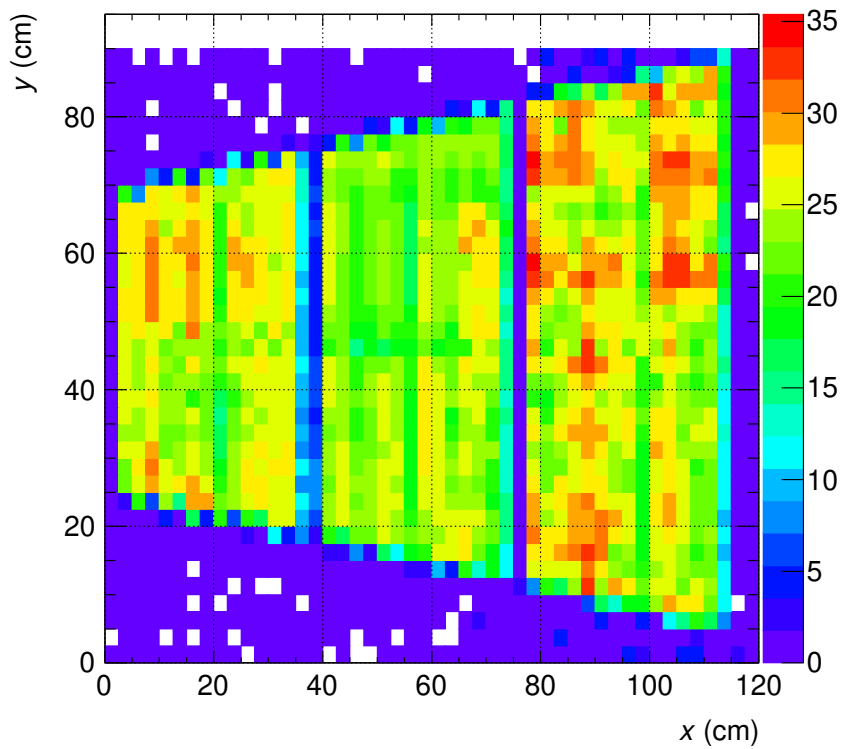


Figure 12. The pad current (in nA) as a function of the position of the x-ray tube for chamber OROC/23. The gain uniformity is 11% (standard deviation), well below the requirement of 20%.

100 The ion backflow (IBF) measurement is performed in parallel with the gain uniformity test.
 101 For this purpose, the cathode current is recorded along with the pad one. The cathode current
 102 is caused by ions traversing the drift volume and reaching the cathode. The IBF factor is
 103 calculated as the ratio between the cathode and the pad currents. An example map is shown in
 Fig. 13.

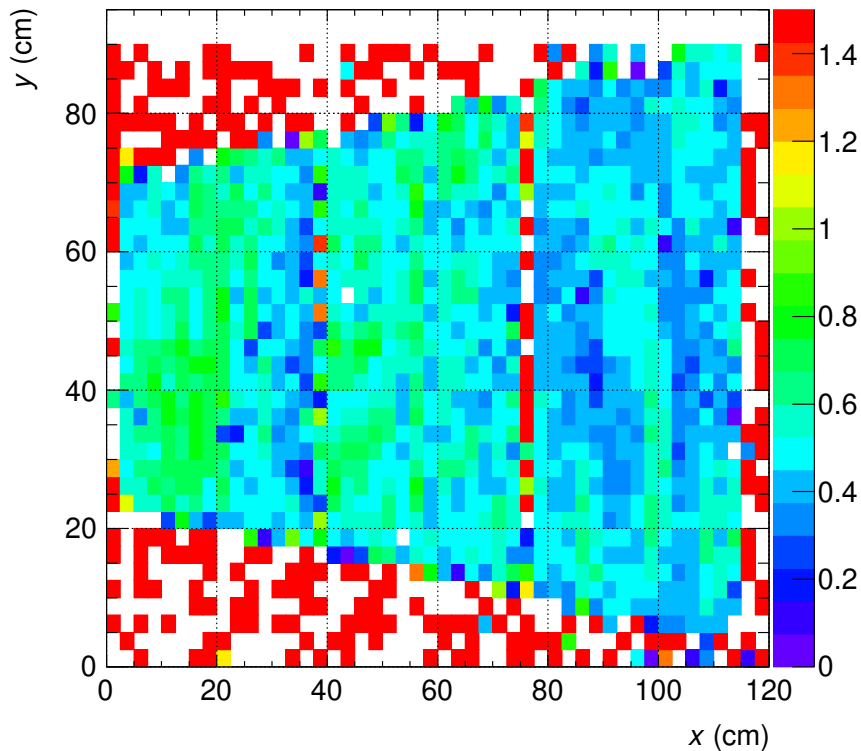


Figure 13. The ion backflow factor (in percent) as a function of the position of the x-ray tube for chamber OROC/23. The IBF factor was calculated as the ratio between the cathode and pad currents. Its mean value is 0.5%, well below the required limit of 1%.

104 The stability of each chamber was checked by illuminating it semi-uniformly with two strong
 105 x-ray tubes. The level of irradiation was such that the pad current was 10 nA/cm^2 and the test
 106 duration was 6 hours. The pad and cathode currents were monitored. After the test, the health
 107 of all GEMs was checked by measuring their dark currents.

108 Upon completion of the tests, each chamber was enclosed in its transportation box. The gas
 109 tightness was checked and the boxes were flushed with nitrogen. After the last check of the
 110 GEM integrity, performed by applying 250 V to each GEM and measuring its dark current, the
 111 chambers were shipped to CERN.
 112

113 4. GEM chamber installation

114 In the beginning of 2019, the ALICE TPC was extracted and brought to a dedicated cleanroom
 115 on the surface. The replacement of the chambers started in April and was completed in
 116 September. Installation of a chamber requires inserting it into the TPC, turning, and pressing
 117 from inside against the backplate (Fig. 14). The removal of wire chambers and the installation
 118 of GEM chambers each proceeded at a pace of two sectors per day. Replacing all 72 chambers
 119 took six months.

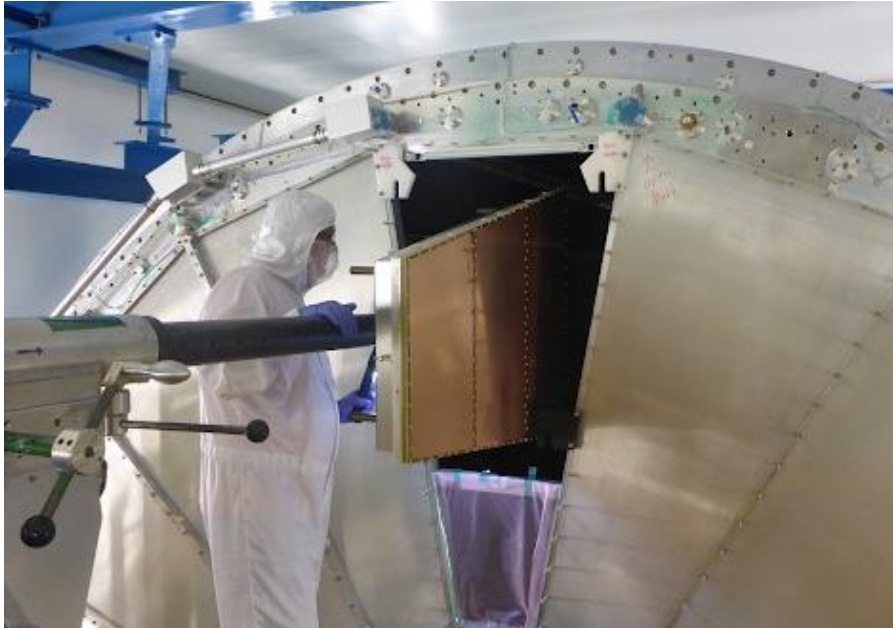


Figure 14. Chamber replacement in the ALICE TPC. The operation took six months and was performed in a dedicated cleanroom at CERN.

5. Concluding remarks

The involvement of the GSI group in the construction of the GEM chambers for the ALICE TPC upgrade started in 2015 with planning, ordering equipment, and defining procedures. The peak production took place in 2017–2018. With the new GEM technology and large detector sizes, the production encountered several surprises and some procedures had to be adjusted correspondingly. In all production steps, strong emphasis was put on quality assurance.

The works were performed in the GSI detector laboratory. It was a privilege and pleasure to use its excellent infrastructure. Our hosts, the detlab colleagues, were welcoming and helped to quickly overcome some of the encountered problems. We appreciate their purely science- and curiosity-driven motivation and gratefully acknowledge their contribution to our project.

By the end of 2019, the time of submission of these proceedings, the chambers have been installed in the TPC, and the TPC commissioning has just started. We are all looking forward to seeing the upgraded TPC performing beautifully in the coming LHC Run 3.

References

- [1] Alme J *et al* 2010 The ALICE TPC, a large 3-dimensional tracking device with fast readout for ultra-high multiplicity events *Nucl. Instrum. Meth.* **A622** 316-367
- [2] Aamodt K *et al.* [ALICE Collaboration] 2008 The ALICE experiment at the CERN LHC *JINST* **3** S08002
- [3] Abelev B *et al.* [ALICE Collaboration] 2014 Performance of the ALICE Experiment at the CERN LHC *Int. J. Mod. Phys. A* **29** 1430044
- [4] ALICE Collaboration 2013 Upgrade of the ALICE Time Projection Chamber *CERN-LHCC-2013-020*, *ALICE-TDR-016*
- [5] ALICE Collaboration 2015 Addendum to the Technical Design Report for the Upgrade of the ALICE Time Projection Chamber *CERN-LHCC-2015-002*, *ALICE-TDR-016-ADD-1*